Effects of chemical reaction on MHD mixed convection stagnation point flow toward a vertical plate in a porous medium with radiation and heat generation

Effects of chemical reaction on MHD mixed convection stagnation point flow toward a vertical plate in a porous medium with radiation and heat generation

Niranjan Hari[1], S Sivasankaran[1], M Bhuvaneswari[2] and Zailan Siri[1]

[1]Institute of Mathematical Sciences, University of Malaya, Kuala Lumpur 50603, Malaysia.
[2]Department of Mechanical Engineering, University of Malaya, Kuala Lumpur 50603, Malaysia.

E-mail: sd.siva@yahoo.com

Abstract. The aim of the present study is to analyze the effects of chemical reaction on MHD mixed convection with the stagnation point flow towards a vertical plate embedded in a porous medium with radiation and internal heat generation. The governing boundary layer equations are transformed into a set of ordinary differential equations using similarity transformations. Then they are solved by shooting technique with Runge-Kutta fourth order iteration. The obtained numerical results are illustrated graphically and the heat and mass transfer rates are given in tabular form. The velocity and temperature profiles overshoot near the plate on increasing the chemical reaction parameter, Richardson number and magnetic field parameter.

1. Introduction

The study of combined free and forced convection flow of an incompressible viscous fluid with simultaneous heat and mass transfer past a vertical plate under the influence of a magnetic field and chemical reaction has huge applications in water and air pollutions, fibrous insulation, several manufacturing processes of industry such as polymers, aerodynamic extrusion of plastic sheets, etc. A stagnation point is a point in a flow field where the local velocity of the fluid is zero. Boutros et al. [1] explored the steady two-dimensional stagnation point flow of an incompressible viscous fluid over a stretching sheet embedded in a fluid saturated porous medium. Mahapatra and Gupta [2] examined the steady two-dimensional stagnation point flow of an incompressible electrically conducting viscous fluid over a flat deformable sheet. They observed that the wall shear stress increases with increase in magnetic field parameter. Merikin and Pop [3] studied the unsteady free convection boundary layer flow in a porous medium for small and large values of the amplitude of the surface temperature oscillations. Takhar et al. [4] studied magneto mixed convection flow of a viscous incompressible electrically conducting fluid in the vicinity of an axisymmetric stagnation point adjacent to a heated vertical surface. Ferdows et al. [5] numerically investigated the natural convection heat transfer in an inclined semi-infinite plate in a porous medium. They observed that the temperature increases and the velocity of the fluid decreases with increasing the porosity parameter.

The research of MHD incompressible viscous flow has many engineering applications such as a power generator, cooling of reactors, design of heat exchangers and MHD accelerators. Yih [6]numerically analyzed the effect of heat source on steady two dimensional laminar MHD mixed convection flow in a porous medium over a vertical permeable flat plate. Layek et al. [7] analyzed the structure of boundary layer stagnation point flow over a stretching sheet in a porous medium with heat generation and suction/blowing. Bhattacharyya and Layek [8] studied the stagnation-point steady boundary layer flow over a porous shrinking sheet subjected to applied suction and radiation. Afify and Elagazery [9] numerically examined the stagnation point flow, heat and mass transfer of an incompressible, electrically conducting fluid towards a stretching sheet in a porous medium in the presence of chemical reaction. The temperature profile increases with an increase in heat source or sink parameter. They observed that concentration profile increases with an increase in chemical reaction. Chao et al. [10] investigated the chemically reactive stagnation point flow in a catalytic porous bed. Lee et al. [11] investigated heat transfer and fluid flow in a saturated porous medium by using Lie group analysis. They found that the thermal and momentum boundary layer thicknesses increase with increasing radiation parameter. Bhuvaneswari et al. [12] obtained the effects of radiation, internal heat generation on natural convective flow over an inclined surface in a porous medium. When the heat generation parameter increases, the temperature and velocity profiles increase. Bhuvaneswari et al. [13] examined the heat and mass transfer of an incompressible viscous fluid in a semi-infinite inclined surface by using Lie group analysis with chemical reaction. They observed that while increasing the chemical reaction parameter and Schmidt number the thickness of the momentum boundary layer increases. Singh et al. [14] investigated the heat and mass transfer of a mixed convection stagnation point flow through porous media in the presence of the volumetric rate of heat generation/absorption. Mankinde [15] examined the effects of thermal radiation on hydromagnetic mixed convection stagnation point flow with internal heat generation. The present study extends the work of Makinde [15] to include chemical reaction effect on MHD mixed convection stagnation point flow of a vertical plate embedded in a porous medium.

2. Mathematical model

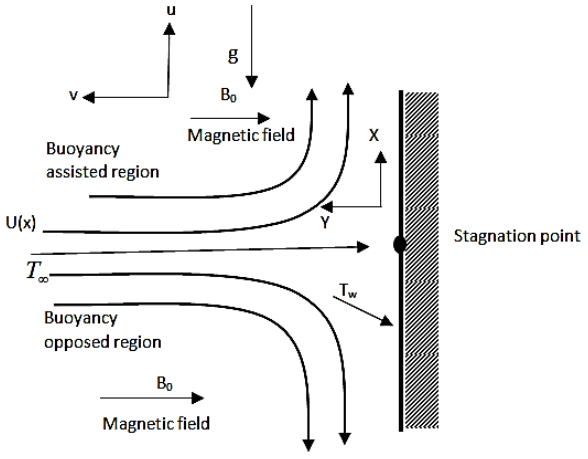

Figure 1. Schematic diagram of the problem.

Consider the two-dimensional steady stagnation-point flow, heat and mass transfer of an incompressible, electrically conducting fluid through a porous medium along a vertical isothermal

plate in the presence magnetic field, volumetric heat generation/absorption and first order homogeneous chemical reaction. The magnetic field of constant strength is imposed along the y-axis. The induced magnetic field is neglected. As the fluid hits the wall at the stagnation point, the flow divided into two streams and the viscous flow adheres to the plate within the boundary layer. The velocity distribution in the potential region flow is assumed as $U_\infty = cx$, where c is a positive constant. The following equations represent the flow in a porous medium obeying the Darcy law. Thus, the governing equations of continuity of mass, momentum transfer, energy transfer and species concentration are given by

$$\frac{\partial u}{\partial x} + \frac{\partial v}{\partial y} = 0, \tag{1}$$

$$u\frac{\partial u}{\partial x} + v\frac{\partial u}{\partial y} = \upsilon\frac{\partial^2 u}{\partial y^2} + g\beta(T - T_\infty) + g\beta^*(C - C_\infty) - \Big(\frac{\sigma_\varepsilon B_0^2}{\rho} + \frac{\upsilon}{\tilde{K}}\Big)(u - U_\infty) + U_\infty\frac{dU_\infty}{dx}, \tag{2}$$

$$u\frac{\partial T}{\partial x} + v\frac{\partial T}{\partial y} = \alpha\frac{\partial^2 T}{\partial y^2} - \frac{\alpha}{k}\frac{\partial q_r}{\partial y} + Q(T - T_\infty), \tag{3}$$

$$u\frac{\partial C}{\partial x} + v\frac{\partial C}{\partial y} = D\frac{\partial^2 C}{\partial y^2} - \Gamma_0(C - C_\infty). \tag{4}$$

The boundary conditions are

$$\begin{aligned} u = 0, \quad v = 0, \quad T = T_w, \quad C = C_w \ \text{ at } \ y = 0, \\ u \to U_\infty = cx, \quad T \to T_\infty, \quad C \to C_\infty, \ \text{ as } \ y \to \infty, \end{aligned} \tag{5}$$

where u and v are the components of velocity along x and y directions, respectively, g, $\tilde{K}$, υ, σ_ε, β, β^*, T, c_p, α, k, Q, B_0, D, T_w, and Γ_0 are gravitational acceleration, permeability of the porous medium, kinematic viscosity, electrical conductivity, thermal expansion coefficient, coefficient of concentration expansion, temperature, thermal diffusivity, thermal conductivity, volumetric heat generation/absorption, strength of magnetic field, mass diffusivity, temperature of the plate and chemical reaction rate of solutal concentration. The chemical reaction is taking place at the wall and the substance generated due to chemical reaction is represented as concentration C. The medium is assumed as grey and transparent. It absorbs heat and emits and dispersion of heat are very small. Hence the radiation effect is taken in the medium due to Stefan Boltzmann's law which states that the radiation is proportional to the 4^{th} power of temperature. Heat flux due to radiation is given by,

$$q_r = -\frac{4\sigma^*}{3K'}\frac{\partial T^4}{\partial y}, \tag{6}$$

where σ^* and K' are the Stefan-Boltzmann constant and the mean absorption coefficient, respectively. Using the Rosseland approximation, it is assumed that the differences in temperature within the flow are too small, so that, using Taylor series T^4 may be shown as a

linear function of temperature T about the free stream temperature T_∞ i.e., T^4 is approximately $4T_\infty^3 T - 3T_\infty^4$. Then we get

$$q_r = -\frac{16\sigma^* T_\infty^3}{3K'}\frac{\partial T}{\partial y}. \tag{7}$$

Equation (7) is substituted in (3) for temperature. We introduce the following non-dimensional variables:

$$\eta = y\sqrt{\frac{c}{\upsilon}},\ \Psi(x,y) = \sqrt{\upsilon c}\, x f(\eta),\ Cr = \frac{\Gamma_0}{c},\ \theta(\eta) = \frac{T - T_\infty}{T_\omega - T_\infty},$$
$$\phi(\eta) = \frac{C - C_\infty}{C_\omega - C_\infty},\ Gr_T = \frac{g\beta(T_\omega - T_\infty)x^3}{\upsilon^2},\ Gr_c = \frac{g\beta^*(C_\omega - C_\infty)x^3}{\upsilon^2},$$
$$Ri_T = \frac{Gr_T}{Re_x^2},\ Ri_C = \frac{Gr_c}{Re_x^2},\ Re_x = \frac{U_\infty x}{\upsilon},\ Rd = \frac{4\sigma^* T_\infty^3}{kK'},\ K = \frac{\upsilon}{c\tilde{K}},$$
$$Pr = \frac{\upsilon}{\alpha},\ Sc = \frac{\upsilon}{D},\ M = \frac{\sigma_\varepsilon B_0^2}{c\rho},\ S = \frac{Q\upsilon}{\alpha c} = Pr\frac{Q}{c}, \tag{8}$$

where Ψ is the stream function which is defined in the usual form as $u = \frac{\partial \Psi}{\partial y}$ and $v = -\frac{\partial \Psi}{\partial x}$ so that the continuity equation (1) is automatically satisfied. Substituting the expression in (7) together with the variables in (8) into (1)-(5), we obtain the following nonlinear ordinary differential equations:

$$f''' + ff'' - f'^2 + Ri_T\theta + Ri_c\phi - (K + M)(f' - 1) + 1 = 0, \tag{9}$$

$$\left(1 + \frac{4}{3}Rd\right) + Prf\theta' + S\theta = 0, \tag{10}$$

$$\phi'' + Scf\phi' - ScCr\phi = 0, \tag{11}$$

where Cr is a chemical reaction parameter, Gr_c is solutal Grashof number, Gr_T is thermal Grashof number, K is a porous medium permeability parameter, M is magnetic field parameter, Pr is Prandtl number, Rd is a thermal radiation parameter, Ri_c is the solutal Richardson number, Ri_T is the thermal Richardson number, S is an internal heat generation/absorption parameter, Sc is Schmidt number. The corresponding boundary conditions (5) are

$$f = 0,\quad f' = 0,\quad \theta = 1,\quad \phi = 1,\ \text{ as }\ \eta = 0,$$
$$f' = 1,\quad \theta = 0,\quad \phi = 0,\ \text{ as }\ \eta \to \infty. \tag{12}$$

The set of equations (9)-(11) with the boundary conditions (12) has been solved numerically by applying the shooting technique along with fourth order Runge-Kutta integration scheme.

The skin friction (C_f) is the force along the surface, the Nusselt number (Nu) represents heat transfer through a fluid as a result of convection relative to conduction across the same fluid layer. The Sherwood number (Sh) is the ratio between the convective to diffusive mass transfer. These nondimensional numbers $C_f,\ Nu,\ Sh$ are defined as follows,

$$C_f = \frac{2\tau_\omega}{\rho U_\infty^2},\quad Nu = \frac{xq_\omega}{k(T_\omega - T_\infty)},\quad Sh = \frac{xq_m}{D(C_\omega - C_\infty)}, \tag{13}$$

$$\tau_\omega = \mu \frac{\partial u}{\partial y}\Big|_{y=0},\ q_\omega = -k\frac{\partial T}{\partial y}\Big|_{y=0} - \frac{4\sigma^*}{3K'}\frac{\partial T^4}{\partial y}\Big|_{y=0},\ q_m = -D\frac{\partial C}{\partial y}\Big|_{y=0}. \tag{14}$$

Substituting (7), (8) and (13) into (14), we obtain the expressions for the skin-friction coefficient, the local Nusselt number and the local Sherwood number as follows.

$$Re_x^{\frac{1}{2}} C_f = f''(0),\ Re_x^{\frac{1}{2}} Nu = -(1+4Rd/3)\theta'(0),\ Re_x^{\frac{1}{2}} Sh = -\phi'(0). \tag{15}$$

The accuracy of our numerical procedure is tested by directly comparing with the previously published work of Singh et al. [14] and Makinde [15] for special cases of the problem under consideration. Table 1 shows that the complete agreement between the comparison results exists. This gives confidence in the numerical results to be reported subsequently.

Table 1. Computation showing the comparison with Singh el al. [14] and Makinde [15] for different values of S when $Ri_T = 1$, $Ri_C = 0.5$, $Pr = 1$, $Sc = 0.5$, $M = 0$, $K = 0$, $Cr = 0$, $Rd = 0$.

	$f''(0)$			$-\theta'(0)$			$-\phi'(0)$		
S	Singh [14]	Makinde [15]	Present	Singh [14]	Makinde [15]	Present	Singh [14]	Makinde [15]	Present
-1	1.8444	1.8444	1.8501	1.3908	1.3908	1.3897	0.4631	0.4631	0.4618
0	1.9995	1.9995	1.9989	0.6392	0.6932	0.6401	0.4789	0.4789	0.4761
1	2.1342	2.1342	2.1299	-0.0730	-0.0730	-0.0727	0.4917	0.4917	0.4902

3. Results and discussions

The results are displayed graphically for different parameters $(K, M, Ri_T, Ri_c, S, Rd, Cr)$, with $Pr = 0.7$ (air) and $Sc = 0.5$. Table 2 illustrates the effect of skin friction, Nusselt number and Sherwood number of different parameters. The skin friction increases with increasing porous medium permeability parameter, magnetic field perimeter and it decreases with increasing the chemical reaction parameter. The local Nusselt number increases with an increasing permeability parameter, magnetic field parameter, thermal radiation parameter and decreases with increasing Richardson number, heat generation parameter. The local Sherwood number increases with an increasing permeability parameter, magnetic field parameter, Richardson number, internal heat generation, chemical reaction parameter.

Figure 2 shows the velocity profiles for different values of K with constant $Ri_T = 1$, $Ri_c = 0.5$, $M = 0.5$, $Rd = 0.2$, $S = 0.2$, $Cr = 0.2$. Figure 2 shows that the fluid velocity increases gradually from the stationary plate surface to its peak value. It is clear that an overshoot in the fluid velocity towards the plate surface is observed. The velocity of the fluid decreases with an increase in the porous medium permeability parameter (K). Figure 3 depicts the influence of different magnetic field parameter values of the velocity field discussed with constant $Ri_T = 1$, $Ri_c = 0.5$, $K = 0.5$, $Rd = 0.2$, $S = 2$, $Cr = 0.2$ values. It is seen from this figure that the velocity decreases initially and then increases with increasing the magnetic field intensity. Boundary layer thickness is very high near the plate.

It is observed from the Figures 4 & 5 that velocity increases as the Richardson number increases. The fluid motion is enhanced by buoyancy forces with increasing values of solutal and thermal (Ri_c, Ri_T) Richardson numbers leading to velocity overshoots near the plate within the boundary layer. The fluid velocity increases gradually from the stationary plate surface

to its peak value within the boundary layer region for different values of S with constant Ri_T, Ri_c, K, M, Rd, Cr, see Figure 6. Figures 7 illustrate the temperature profiles for different values of S. We can observe that thermal boundary layer thickness is more than the momentum boundary layer thickness. It is observed from Figure 8 that the temperature increases

Table 2. Different values of f'', $-\theta'$, $-\phi'$ for $Pr = 0.7$ and $Sc = 0.5$.

K	M	Ri_T	Ri_C	S	Rd	Cr	$f''(0)$	$-\theta'(0)$	$-\phi'(0)$
0	0.5	1	0.5	0.2	0.2	0.2	2.282218	0.129818	0.565269
0.5							2.381054	0.131488	0.566446
1.0							2.480144	0.132527	0.567637
2.0							2.658150	0.133415	0.570214
3.0							2.818487	0.134906	0.572237
0.5	0	1	0.5	0.2	0.2	0.2	2.282218	0.129818	0.565269
	2						2.658150	0.133415	0.570214
	4						3.050930	0.139619	0.572251
	6						4.249084	0.157870	0.565790
	8						5.507522	0.135105	0.581117
0.5	0.5	0.1	0.5	0.2	0.2	0.2	1.875287	0.138825	0.546017
		0.5					2.101744	0.135415	0.555178
		1.0					2.381054	0.131488	0.566446
		1.5					2.656359	0.127927	0.577511
		2.0					2.927848	0.124727	0.588375
0.5	0.5	1	0.1	0.2	0.2	0.2	2.203743	0.132965	0.559868
			0.5				2.381054	0.131488	0.566446
			1.0				2.598403	0.129982	0.574389
			1.5				2.811546	0.128839	0.582031
			2.0				3.021085	0.128045	0.589378
0.5	0.5	1	0.5	-1.0	0.2	0.2	2.277775	0.675466	0.561458
				-0.5			2.313538	0.479968	0.563299
				0.0			2.359292	0.242043	0.565472
				0.5			2.418090	-0.054742	0.568029
				1.0			2.493639	-0.432447	0.571028
0.5	0.5	1	0.5	0.2	0	0.2	2.380285	0.11306	0.565899
					0.2		2.381054	0.131488	0.566446
					0.4		2.380925	0.143412	0.566865
					0.8		2.380485	0.177186	0.567461
					1.0		2.381412	0.27606	0.567570
0.5	0.5	1	0.5	0.2	0.2	-1.0	2.425714	0.130183	0.036520
						-0.5	2.404500	0.130797	0.284168
						0	2.387099	0.131309	0.492312
						0.5	2.372845	0.131731	0.669348
						1.0	2.361162	0.132074	0.822065

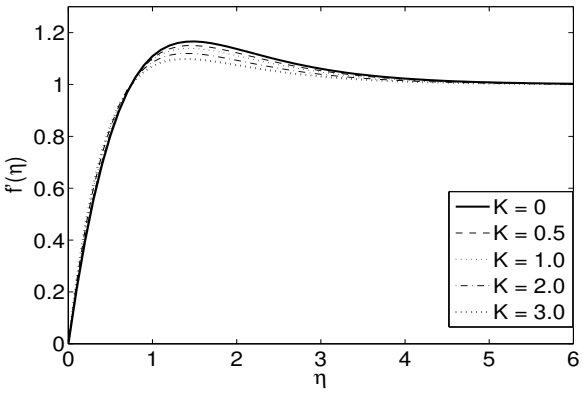

Figure 2. Velocity profiles for different K values with $Ri_T = 1$, $Ri_C = 0.5$, $M = 0.5$, $Rd = 0.2$, $S = 0.2$, $Cr = 0.2$.

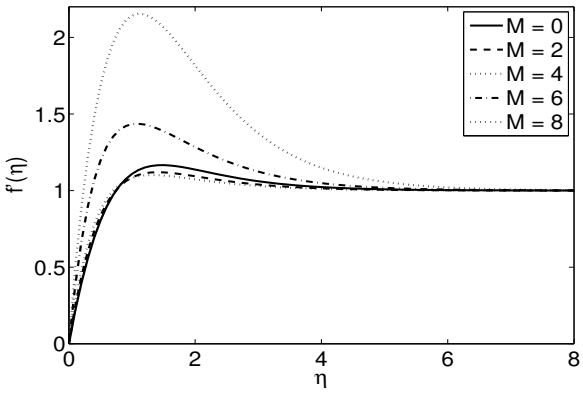

Figure 3. Velocity profiles for different M values with $Ri_T = 1$, $Ri_C = 0.5$, $K = 0.5$, $Rd = 0.2$, $S = 0.2$, $Cr = 0.2$.

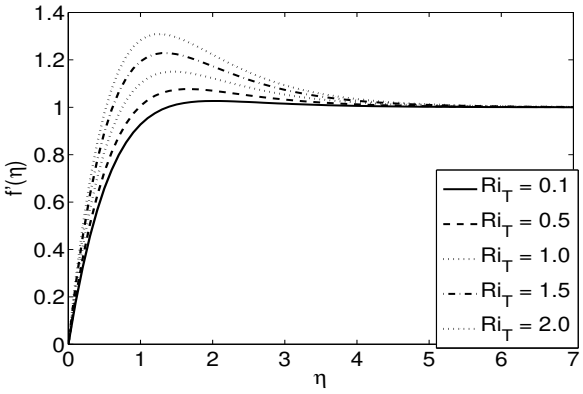

Figure 4. Velocity profiles for different Ri_T values with $Ri_C = 0.5$, $K = 0.5$, $M = 0.5$, $Rd = 0.2$, $S = 0.2$, $Cr = 0.2$.

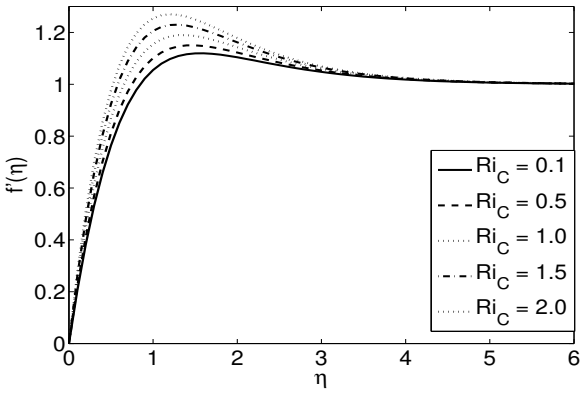

Figure 5. Velocity profiles for different Ri_C values with $Ri_T = 1$, $K = 0.5$, $M = 0.5$, $Rd = 0.2$, $S = 0.2$, $Cr = 0.2$.

with increasing the thermal radiation parameter. Figure 9 illustrates the concentration profiles for different Cr values with constant Ri_T, Ri_c, K, M, S, Rd values. We observe that the concentration gradually decreases exponentially in the boundary layer on increasing Cr values. At the plate surface contains a high chemical species concentration and decay exponentially far away from the plate.

4. Conclusion

In this paper, we studied the MHD mixed convection stagnation point flow, heat and mass transfer toward a vertical plate in a porous medium with radiation, internal heat generation and chemical reaction. The main findings are summarized as follows: The velocity profiles overshoot near the plate surface on increasing the magnetic field, Richardson number and internal heat generation parameter. The velocity decreases on increasing the porous medium permeability parameter. The temperature increases with an increase in the heat generation and thermal radiation parameters. The concentration decreases on increasing the chemical reaction parameter.

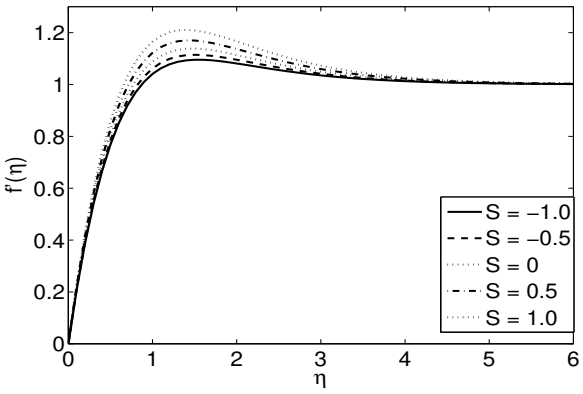

Figure 6. Velocity profiles for different S values with $Ri_T = 1$, $Ri_C = 0.5$, $K = 0.5$, $M = 0.5$, $Rd = 0.2$, $Cr = 0.2$.

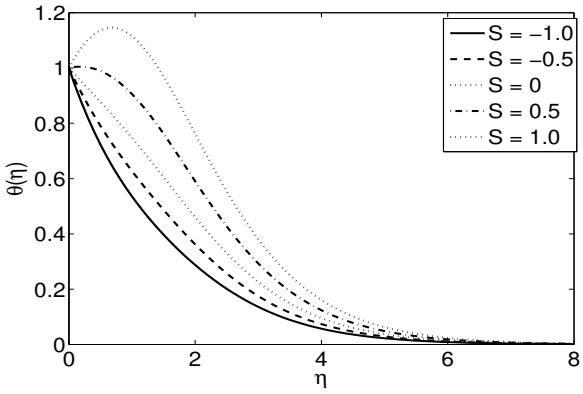

Figure 7. Temperature profiles for different S values with $Ri_T = 1$, $Ri_C = 0.5$, $K = 0.5$, $M = 0.5$, $Rd = 0.2$, $Cr = 0.2$.

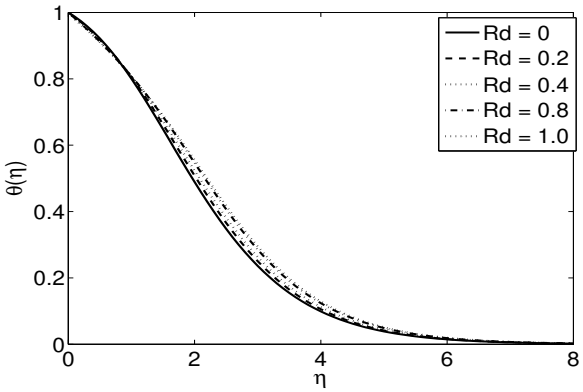

Figure 8. Temperature profiles for different Rd values with $Ri_T = 1$, $Ri_C = 0.5$, $K = 0.5$, $M = 0.5$, $S = 0.2$, $Cr = 0.2$.

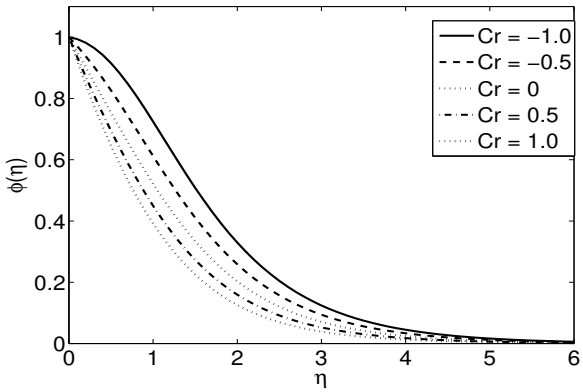

Figure 9. Concentration profiles for different Cr values with $Ri_T = 1$, $Ri_C = 0.5$, $K = 0.5$, $M = 0.5$, $Rd = 0.2$, $S = 0.2$.

Acknowledgments

Authors would like to thank the University of Malaya for the financial support through the research grants, RG216-12AFR and RP011B-13AFR.

References

[1] Boutros Y Z, Malek M B A, Badran N A and Hassan H S 2006 Lie-group method of solution for steady two dimensional boundary layer stagnation point flow towards a heated stretching sheet placed in a porous medium *Meccanica* **41** 681–91

[2] Mahapatra T R and Gupta A S 2000 Magneto hydrodynamic stagnation-point flow towards a stretching sheet *Acta Mechanica* **152** 191–6

[3] Merkin J H and Pop I 2000 Free convection near a stagnation point in a porous medium resulting from an oscillatory wall temperature *Int. J. Heat Mass Transf.* **43** 611–21

[4] Takhar H S, Chamkha A J and Nath G 2003 Unsteady mixed convection on the stagnation point flow adjacent to a vertical plate with a magnetic field *Heat Mass Transf.* **41** 387–98

[5] Ferdows M, Kaino K and Sivasankaran S 2009 Free Convection Flow in an inclined porous surface *J. Porous Media* **12** 997–1003

[6] Yih K A 1998 Heat source/sink effect on MHD mixed convection in stagnation flow on a vertical permeable plate in porous media *Int. Commun. Heat Mass Transf.* **25** 427–42
[7] Layek G C, Mukhopadhyay S and Samad Sk A 2007 Heat and mass transfer analysis for boundary layer stagnation-point flow towards a heated porous stretching sheet with heat absorption/generation and suction/blowing *Int. Commun. Heat Mass Transf.* **34** 347–56
[8] Bhattacharyya K and Layek G C 2010 Effects of suction/blowing on steady boundary layer stagnation-point flow and heat transfer towards a shrinking sheet with thermal radiation *Int. J. Heat Mass Transf.* **54** 302–7
[9] Afify A A and Elagazery Nasser S 2012 Lie group analysis for the effects of chemical reaction on MHD stagnation-point flow of heat and mass transfer towards a heated porous stretching sheet with suction or injection *Nonlinear Analysis: Modelling Control* **17** 1–15
[10] Chao B.H, Wang H and Cheng P 1996 Stagnation point flow of a chemically reactive fluid in a catalytic porous bed *Int. J. Heat Mass Transf.* **39** 3003–19
[11] Lee J, Kandaswamy P, Bhuvaneswari M and Sivasankaran S 2008 Lie group analysis of radiation natural convection heat transfer past an inclined porous surface *J. Mech. Sci. Tech.* **22** 1779–84
[12] Bhuvaneswari M, Sivasankaran S and Kim Y J 2012 Lie group analysis of radiation natural convection flow over an inclined surface in a porous medium with internal heat generation *J. Porous Media* **15** 1155–64
[13] Bhuvaneswari M, Sivasankaran S and Ferdows M 2009 Lie group analysis of natural convection heat and mass transfer in an inclined surface with chemical reaction *Nonlinear Analysis: Hybrid Systems* **3** 536–42
[14] Singh G, Sharma P R and Chamkha A J 2010 Effect of volumetric heat generation/absorption of mixed convection stagnation point flow on an iso-thermal vertical plate in porous media *Int. J. Ind. Math.* **2** 59–71
[15] Makinde O D 2011 Heat and mass transfer by MHD mixed convection stagnation point flow toward a vertical plate embedded in a highly porous medium with radiation and internal heat generation *Meccanica* **47** 1173–84